Supporting Information

Conductive and stable polyphenylene/CNT composite membrane for electrically enhanced membrane fouling mitigation

Huijuan Xie, Haiguang Zhang, Xu Wang, Gaoliang Wei, Shuo Chen, Xie Quan*

Key Laboratory of Industrial Ecology and Environmental Engineering (Ministry of Education, China), School of Environmental Science and Technology, Dalian University of Technology, Dalian 116024, China

Corresponding Author

*****School of Environmental Science and Technology, Dalian University of Technology, Dalian, China

Phone: +86-411-84706140. Fax: +86-411-84706263. E-mail: quanxie@dlut.edu.cn.

Number of Pages (including the cover): 11

Number of Texts: 3

Number of Figures: 19

Number of Tables: 2

Number of References: 3

1. Fabrication of PVA/CNT membrane

Commercial polyvinylidene fluoride hollow fiber membranes (PVDF HFMs) were washed with ethanol and deionized water and then dried at room temperature (20 °C). The carboxyl CNTs were dispersed into deionized water with the CNTs dispersant (1 g/L) to form a uniform CNT dispersion (0.5 mg/mL). The as-prepared CNTs dispersion was vacuum-filtered through the PVDF HFMs to yield CNT membranes (CNTs loadings: 0.585 mg/cm^2). Subsequently, the membranes were immersed into a 0.2 wt% polyvinyl alcohol (PVA, polymerization degree of 1750 ± 50, 99.0%) solution under vacuum-filtration. After filtration, the membranes were soaked into a 1 wt% succinic acid solution for 1 h, then the membranes were rinsed with deionized water and dried at 80 °C for 4 h, according to the previous literature (Du et al., 2020; Wei et al., 2020).

2. Membrane porosity calculation

The porosity was measured by gravimetric method and calculated by the following Eq. (1) (Wei et al., 2015):

$$\varepsilon = \frac{m_2 - m_1}{\rho \times A \times L} \quad (1)$$

where ε is the porosity of the membrane (%), m_2 is the mass of wet membrane (g), m_1 is the mass of dry membrane (g), A is the cross-sectional area of membrane (cm^2), L is the length of membrane (cm), ρ is the density of pure water (g/cm^3, equals to 1 g/cm^3 at the temperature of 25 °C).

3. Membrane cathodic potential test and cyclic voltammetry curve test

The membrane potentials were tested in a three-electrode system. A PP/CNT membrane was served as the working electrode (cathode), a titanium mesh was used as the counter electrode (anode) and an Ag/AgCl saturated electrode as the reference electrode. The electrode distance was set as 5 mm. A 50 mM Na_2SO_4 solution was used as the electrolyte. Besides, the voltages were applied by a DC stabilized power supply, and the potentials were measured by an electrochemical workstation (Chenhua CHI 760E). The test time at each voltage was 200 s.

The cyclic voltammetry (CV) curves were tested in a three-electrode system. A glassy carbon electrode coated with PP/CNT material was served as the working

electrode, a platinum sheet was used as the counter electrode and an Ag/AgCl saturated electrode as the reference electrode. The electrode distance was set as 5 mm. A 50 mM Na_2SO_4 solution was used as the electrolyte. The scanning range was between 0 and –2.5 V vs. Ag/AgCl, and the scanning rate was 100 mV s^{-1}.

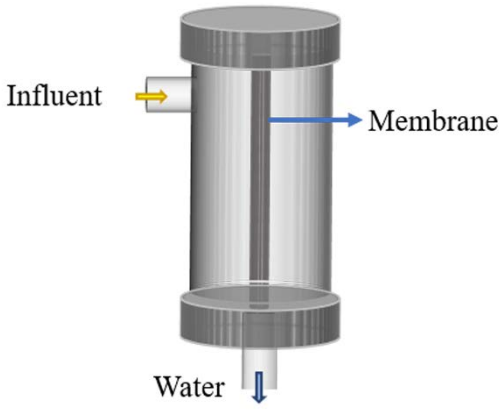

Fig. S1 Diagram of the dead-end filtration membrane module.

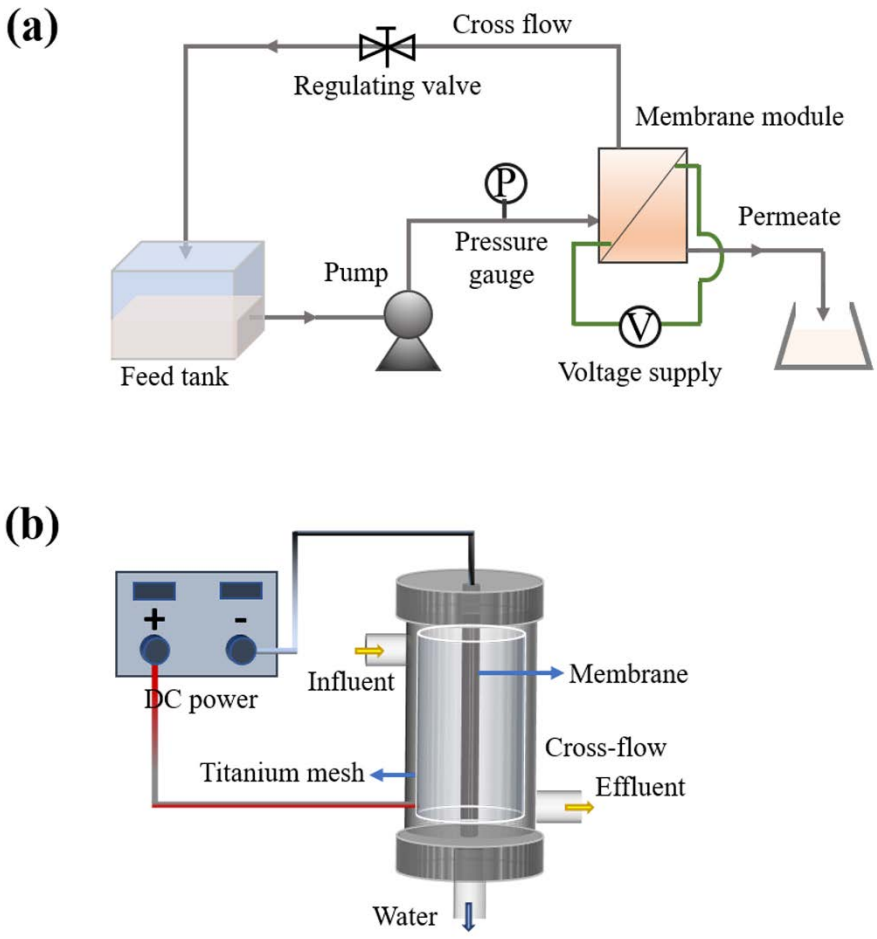

Fig. S2 Diagram of the lab-scale electrical membrane filtration setup and the membrane module.

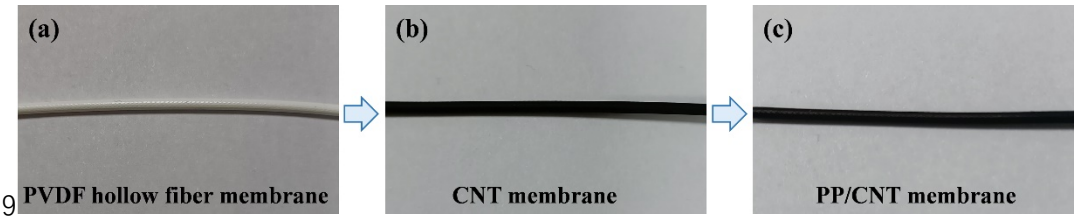

Fig. S3 Photographs of the PP/CNT membrane.

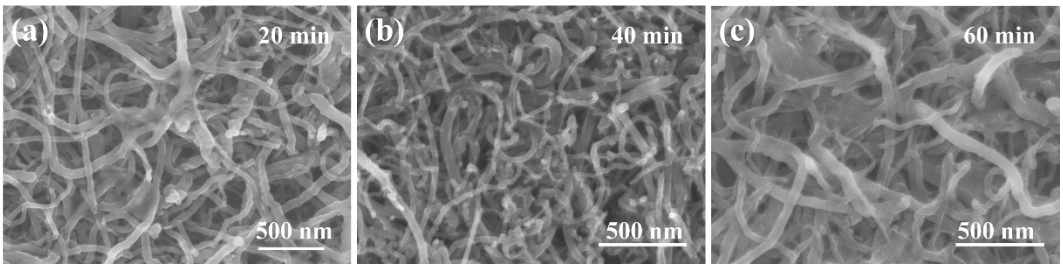

Fig. S4 SEM images of PP/CNT layers with electropolymerization reaction times of (a) 20 min, (b) 40 min, and (c) 60 min.

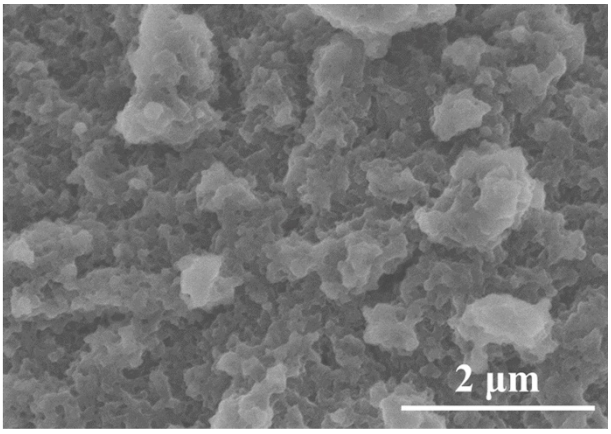

Fig. S5 SEM image of PP.

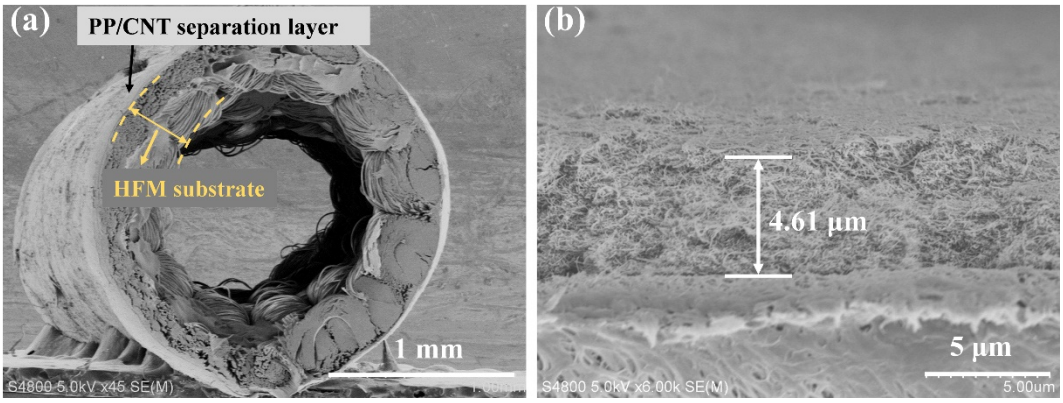

Fig. S6 (a) Cross-section SEM image of the PP/CNT membrane. (b) PP/CNT layer thickness.

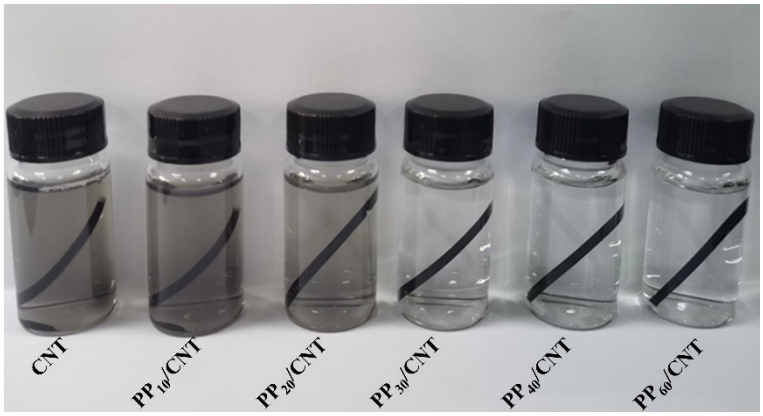

Fig. S7 Photographs of PP_x/CNT membranes with different electropolymerization reaction times (10, 20, 30, 40, 50, and 60 min) after ultrasonic treatment.

Table S1 FTIR band assignments of PP

Location (cm^{-1})	Assignment
3485	O–H stretching vibration
1481	C–C stretching vibration (phenyl ring)
1043	C–C stretching vibration (phenyl ring)
840 (P1)	C–H out-of-plane vibration (adjacent hydrogen atoms on p-disubstituted rings)
752 (P2)	C–H out-of-plane vibration (mono-substituted phenyl ring)
698 (P3)	C–H out-of-plane vibration (mono-substituted phenyl ring)

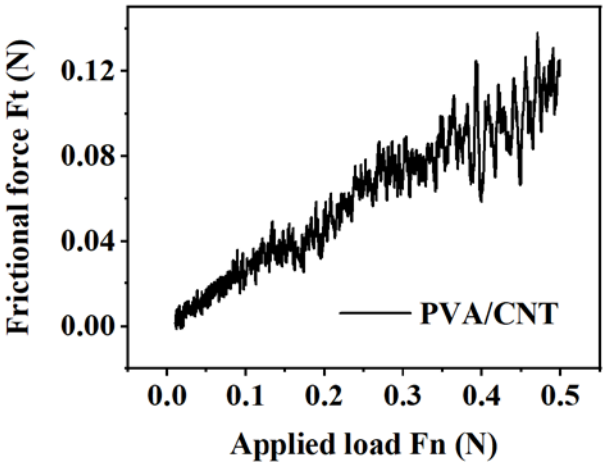

Fig. S8 Nano-scratch result of PVA/CNT membrane.

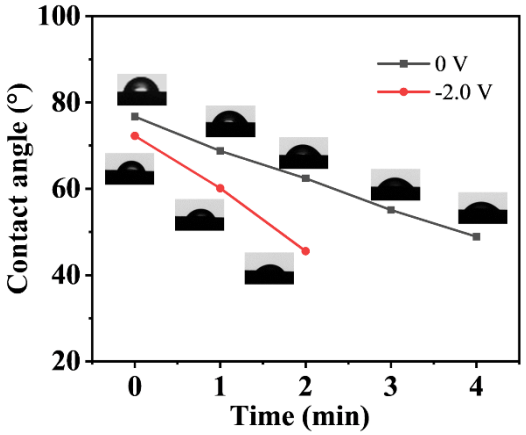

Fig. S9 Time-dependent variations of water contact angles of the PP/CNT membrane at 0 and -2.0 V.

Table S2 Membrane porosities

Membrane	PVDF support	PP/CNT	CNT	CM_1	CM_2	CM_3
Porosity (%)	62 ± 5	80 ± 3	92 ± 2	55 ± 2	57 ± 2	52 ± 6

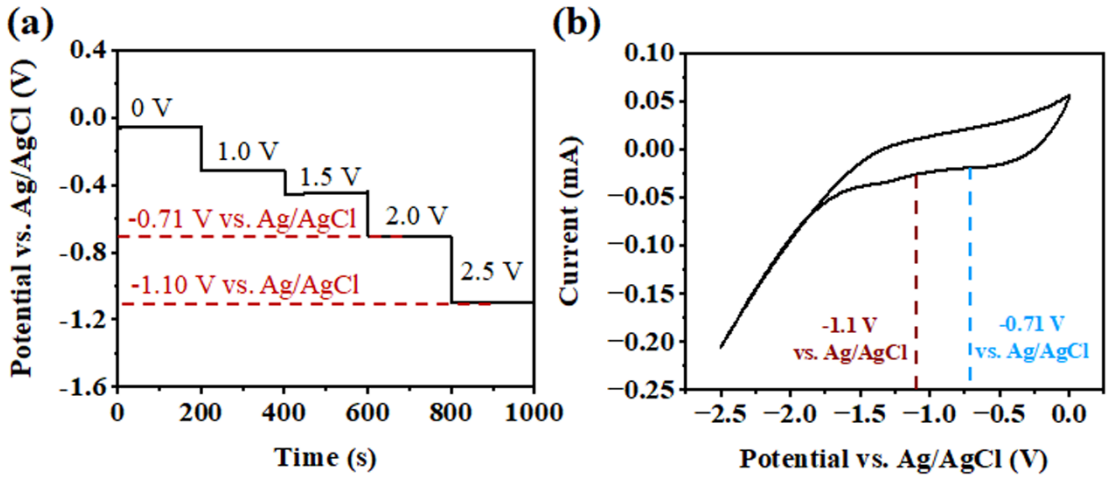

Fig. S10 (a) Membrane cathode potentials (V, vs. Ag/AgCl) as functions of applied voltages from 0 to 2.5V. (b) Cyclic voltammetry (CV) curve of a PP/CNT membrane.

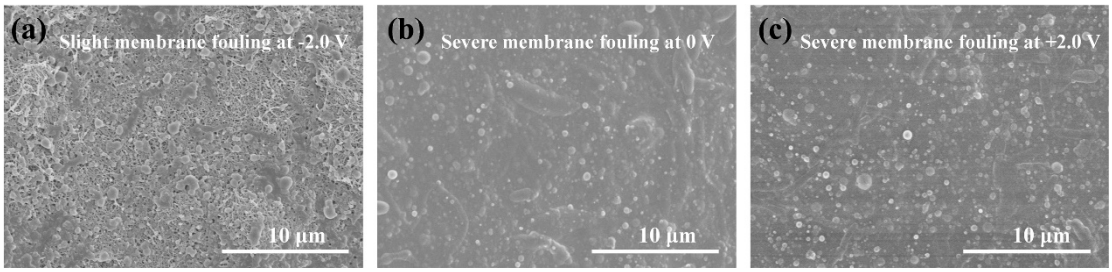

Fig. S11 SEM images of membrane fouling of PP/CNT membranes after SA filtration at the voltages of (a) -2.0 V, (b) 0 V, and (c) +2.0 V.

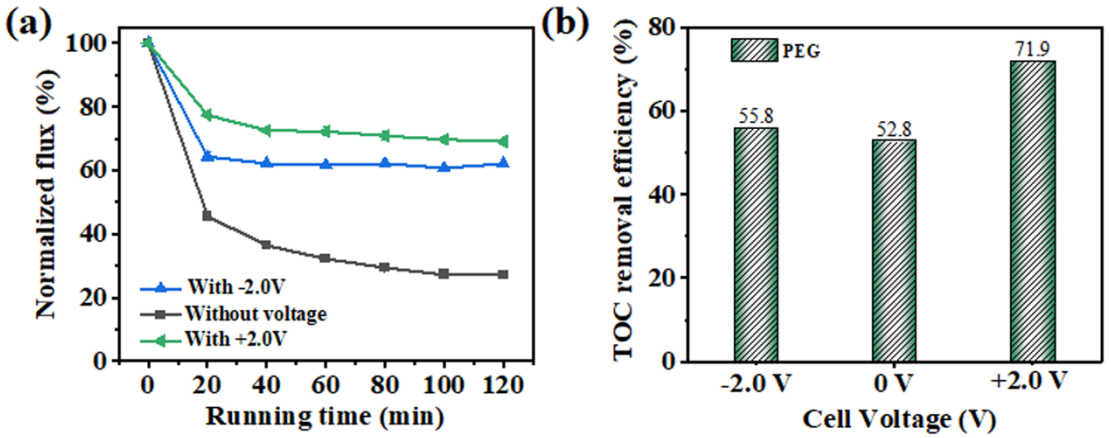

Fig. S12 (a) Normalized fluxes for PEG filtration on the PP/CNT membrane at different cell voltages. (b) PEG removal efficiencies of the PP/CNT membrane at different cell voltages.

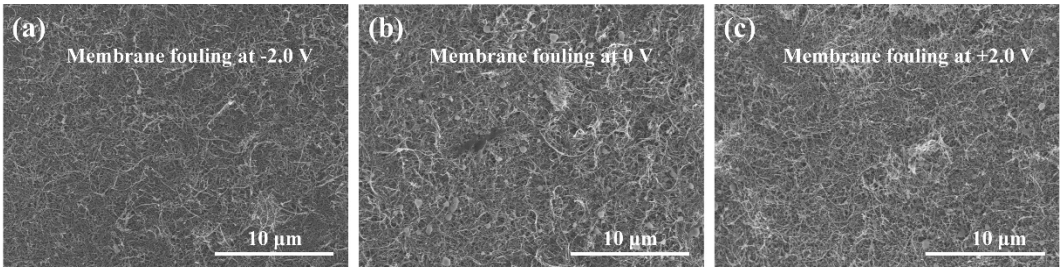

Fig. S13 SEM images of membrane fouling of PP/CNT membranes after PEG filtration at the voltages of (a) -2.0 V, (b) 0 V, and (c) +2.0 V.

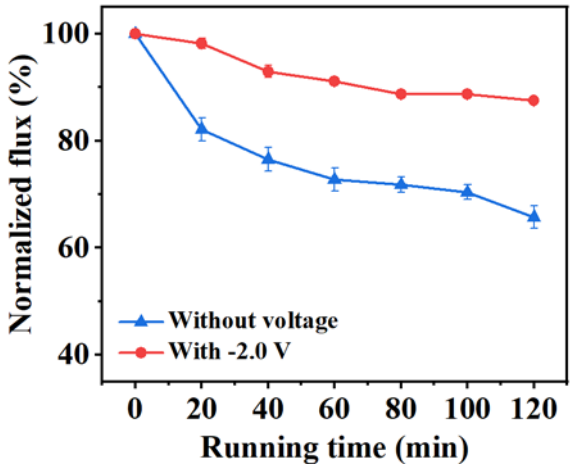

Fig. S14 Normalized fluxes of the PP/CNT membranes with and without electro-assistance when filtrating *E. coli*. solution (operation pressure of 0.2 bar).

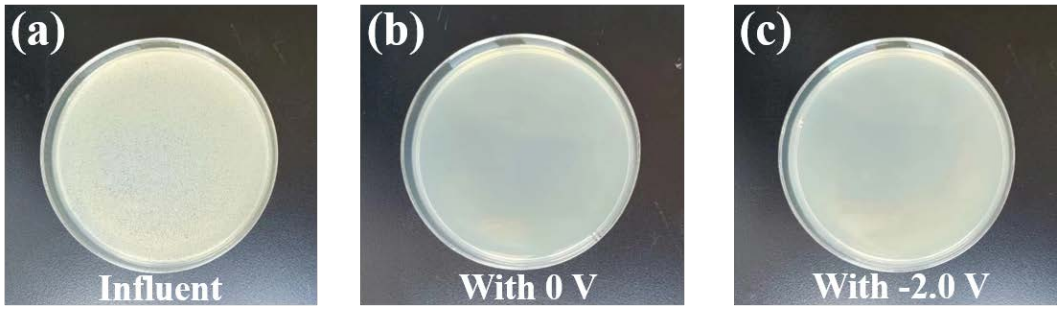

Fig. S15 Photographs of E. coli colonies on the agar plate before and after filtration of *E. coli*. (a) Feed containing *E. coli*. The filtered effluent of PP/CNT membrane at the voltages of (b) 0 V and (c) -2.0 V.

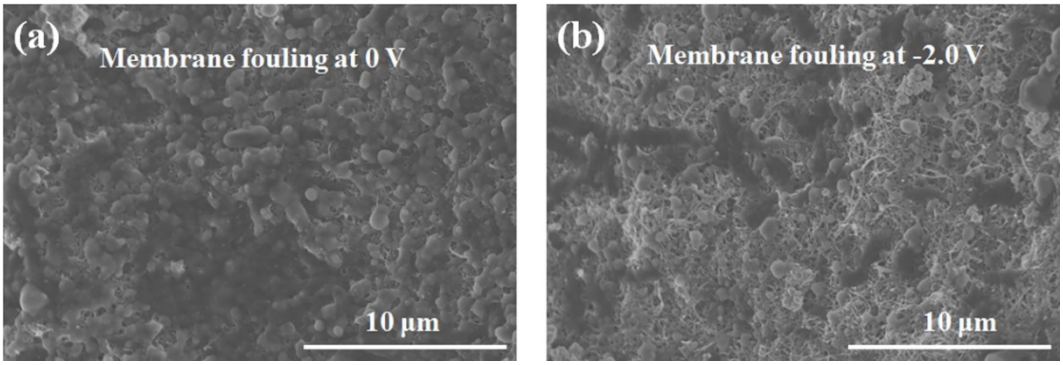

Fig. S16 SEM images of membrane fouling of PP/CNT membranes after *E. coli* filtration at the voltages of (a) 0 V and (b) -2.0 V.

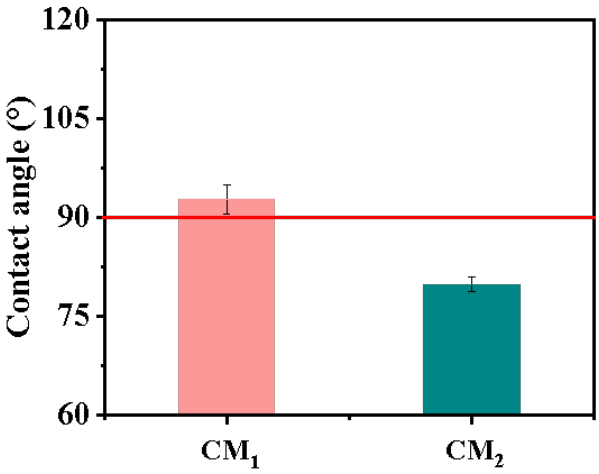

Fig. S17 Water contact angles of the CM_1 and CM_2 membranes.

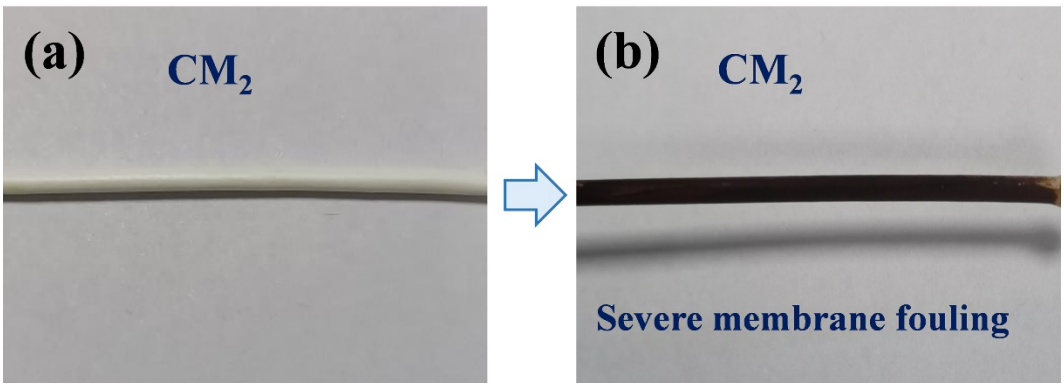

Fig. S18 Photographs of CM_2 membranes (a) before and (b) after HA filtration.

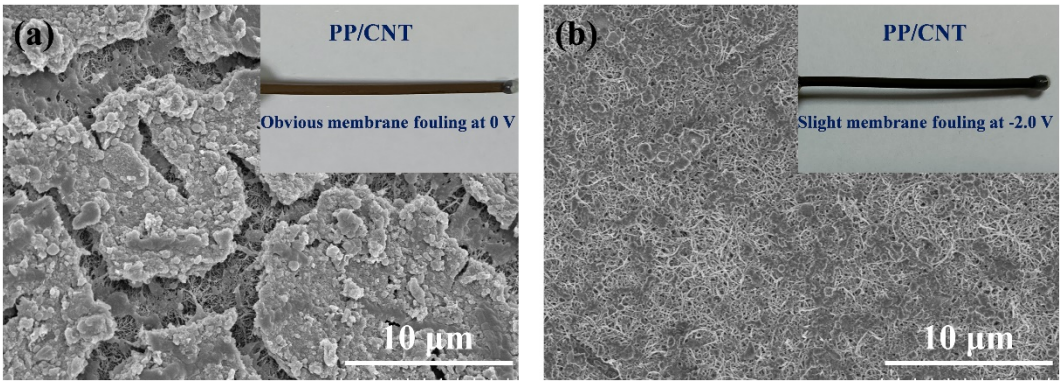

Fig. S19 SEM images of membrane fouling of PP/CNT membranes after HA filtration at the voltages of (a) 0 V and (b) -2.0 V.

References

Du L, Quan X, Fan X, Wei G, Chen S (2020). Conductive CNT/nanofiber composite hollow fiber membranes with electrospun support layer for water purification. Journal of Membrane Science, 596: 117613

Wei G, Chen S, Fan X, Quan X, Yu H (2015). Carbon nanotube hollow fiber membranes: High-throughput fabrication, structural control and electrochemically improved selectivity. Journal of Membrane Science, 493: 97-105

Wei S, Du L, Chen S, Yu H, Quan X (2021). Electro-assisted CNTs/ceramic flat sheet ultrafiltration membrane for enhanced antifouling and separation performance. Frontiers of Environmental Science & Engineering, 15(1): 1-11